Ambient photodoping of p-type organic nanofibers: highly efficient photoswitching and electrical vapor sensing of amines†

Yanke Che,[a] Xiaomei Yang,[a] Zengxing Zhang,[a] Jianmin Zuo,[c] Jeffrey S. Moore*[bc] and Ling Zang*[a]

Received 8th April 2010, Accepted 21st April 2010
First published as an Advance Article on the web 17th May 2010
DOI: 10.1039/c0cc00823k

High photoconductivity of p-type nanofibers fabricated from a reducing tetracyclic macromolecule was achieved though a simple photodoping process under ambient conditions, which, together with the intrinsic high surface area and porosity of the nanofibers when deposited on a substrate, enables application in electrical vapor sensing of organic amines.

One-dimensional (1D) nanomaterials provide speed and sensitivity advantages for applications in chemiresistor based vapor sensing.[1–5] However, most of the 1D nanomaterials reported to date are of an inorganic nature. The limitations of organic counterparts in this emerging field are mainly due to their low intrinsic conductivity. While photodoping (*via* photoinduced electron transfer) has proven to be an effective approach to improve the conductivity of organic materials,[6] only a few such examples have been reported for 1D nanostructures.[7–11] Herein we demonstrate the effective photodoping of p-type organic nanofibers assembled from an alkyl-substituted, carbazole-cornered, arylene-ethynylene tetracyclic macromolecule (TDTC, complete structure shown in SI),[12] and the application of the high photoconductivity thus obtained in vapor sensing of amines (Fig. 1). The elegance of the system lies in the simplicity of the photodoping process, for which the photoinduced electron transfer is initiated between TDTC and the surface adsorbed oxygen under ambient conditions, leaving positive charges (holes) within the nanofiber acting as the major charge carriers.

Fig. 1 shows the SEM image of the nanofibers fabricated from TDTC through a simple solution-based self-assembly (detailed in SI). The obtained nanofibers are *ca.* 20–50 nm in diameter and several micrometres in length. The extended 1D molecular arrangement is likely dominated by the π–π interaction between the planar TDTC molecules (Fig. 1). Such cofacial π–π stacking is clearly indicated by the d-spacing (3.8 Å) as observed in the XRD spectrum (Fig. S1), which corresponds to a regular π–π stacking distance.[12] Electron diffraction from the nanofiber showed a crystal like pattern with sharp diffraction spots (Fig. S2), producing two distinct, reciprocal lattice vectors, giving two d-spacings, d1 = 0.94 nm and d2 = 1.24 nm, which are consistent with the XRD spectrum (Fig. S1). The strong π–π interaction is also consistent with the new absorption band emerged at longer wavelength (centered 377 nm) as measured for the nanofibers in comparison to the molecular solution of TDTC (Fig. S3).

The nanofibers obtained exhibited high conductivity upon irradiation with white light under ambient condition, whereas negligible current was observed in the dark (Fig. 2A). The photoconduction switching has also proven to be reversible with the light turning on and off (Fig. 2B), implying the high stability of the materials when operated under ambient conditions. The high photoconductivity observed is likely correlated to the presence of oxygen, which can usually help increase the concentration of holes for p-type organic materials.[10,13] To confirm the effect of oxygen, we performed the same photocurrent measurements under argon protection (Fig. 2C). Upon introducing an argon atmosphere, the photocurrent gradually decreased, and eventually reached the value measured in the dark. This observation clearly implied that the photoconductivity originated from the photoinduced charge separation between TDTC and oxygen, which is supported by the low ionization potential (*i.e.* high HOMO level) of TDTC.[3] The proposed photoinduced charge separation is consistent with the fluorescence quenching by oxygen observed for the nanofibers, for which the emission intensity decreased about 13% in air compared to that measured under argon (Fig. S4A). There exist two possible mechanisms for the photoinduced charge separation: one is intermolecular electron transfer from the photoexcited state of TDTC to surface adsorbed oxygen,

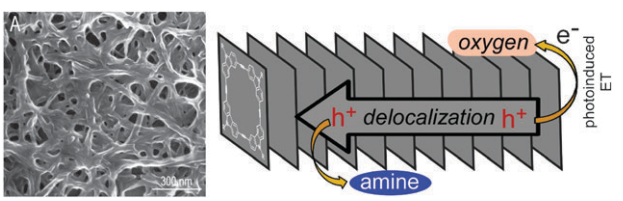

Fig. 1 SEM image (1.2 × 1.2 μm) of entangled TDTC nanofibers deposited on glass; a schematic illustration showing the enhancement of conductivity through photodoping (*i.e.*, photoinduced electron transfer from TDTC to oxygen, leaving holes within the nanofiber) and the decrease in conductivity due to hole depletion by surface-adsorbed amines.

[a] *Department of Materials Science and Engineering, The University of Utah, Salt Lake City, UT 84108, USA. E-mail: lzang@eng.utah.edu; Fax: (+1) 801-585-0625; Tel: (+1) 801-587-1551*
[b] *Department of Chemistry, University of Illinois at Urbana-Champaign, Urbana, IL 61801, USA. E-mail: jsmoore@uiuc.edu; Fax: (+1) 217-244-8024; Tel: (+1) 217-244-4024*
[c] *Department of Materials Science and Engineering, University of Illinois at Urbana-Champaign, Urbana, IL 61801, USA*

† Electronic supplementary information (ESI) available: SEM image, TEM image, XRD data of TDTC nanofibers, *I–V* curves of ACTC nanofibers, optical spectra of ACTC and TDTC nanofibers. See DOI: 10.1039/c0cc00823k

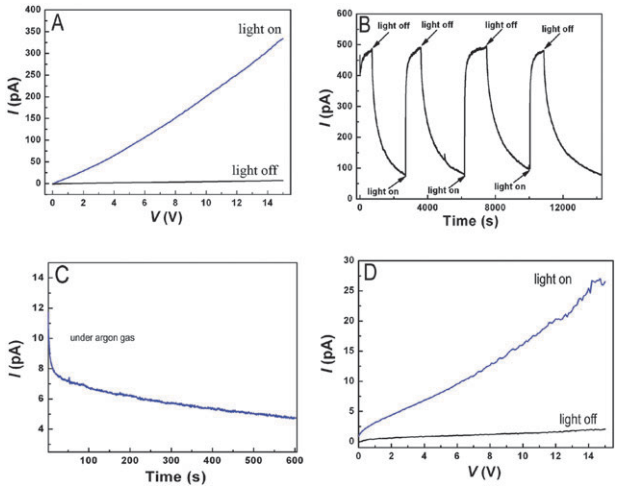

Fig. 2 (A) *I–V* curves measured over TDTC nanofibers in the dark (black) and under white light irradiation at power density of 0.3 mW mm^{-2} (blue); (B) photocurrent (at 10 V) in response to turning on and off the irradiation; (C) photocurrent change (at 10 V) with time following argon gas introduction (monitored 25 min after argon gas started); (D) *I–V* curves measured over a spin-cast film of TDTC in the dark (black) and under the same white light irradiation as used in (A) (blue).

and the other is an intramolecular process within the ground donor–acceptor complex formed between TDTC and oxygen, as previously observed for the reducing conjugated polymers.[14,15]

To further clarify the role played by oxygen in the photocurrent generation, a reference tetracyclic macromolecule, named ACTC (SI),[3] was chosen as the building-block to perform the same investigations for comparison with TDTC. ACTC possesses the same π-skeleton but substituted with acyl-linked alkyl side-chains, which produces almost the same LUMO as that of TDTC, while decreases the HOMO level by as much as 0.7 eV compared to that of TDTC.[3] Although similar nanofibers were fabricated from ACTC using the same method (Fig. S5), negligible photocurrent was generated for these nanofibers under the same irradiation conditions as performed for the TDTC fibers (Fig. S6). Even under irradiation with UV light (to get direct excitation of ACTC), there was still no obvious photocurrent enhancement observed, excluding the possibility of electron transfer from the photoexcited state (*i.e.*, LUMO) of ACTC to oxygen. This is consistent with fluorescence measurements performed on the same nanofibers, for which the presence of oxygen exhibited no influence on the emission intensity of the nanofibers (Fig. S4B). Together these observations suggest that the photocurrent generation in the TDTC nanofibers is due to photoinduced intramolecular charge separation of surface complexes between the TDTC and adsorbed oxygen. The lack of formation of such a ground state complex with ACTC is likely due to its high ionization potential.[3] Generally, the ground state complex formation between oxygen and organic molecules is primarily dependent on the ionization potential of the latter; the lower the ionization potential (or higher HOMO level), the stronger the complexation with oxygen will be.[15]

The cofacial stacking of the TDTC molecules along the long axis of the nanofiber enables long range delocalization of the photogenerated charges similar to other 1D assemblies,[5] thus leading to further enhancement of the conductivity. This is in contrast to the photodoping of film based materials, where the poor intermolecular organization often limits the charge transport. To confirm this argument, we performed the same photocurrent measurement over the spin-cast film of TDTC (Fig. 2D and Fig. S7), for which only slight enhancement of photocurrent was obtained.

Taking advantage of the large surface area and 3D porosity intrinsic to the nanofiber network when deposited onto a substrate in a film format, the nanofibers fabricated from TDTC are expected to function as a chemiresistor for trace vapor sensing of reducing reagents (*e.g.*, amines) through modulation of the electrical current.[2,3] Aniline was chosen as the target analyte here due to its relatively low saturated vapor pressure (allowing for easy dilution down to the ppb range) and its popular use as a precursor in chemical industry. As shown in Fig. 3A, the photoconductivity of the nanofibers is very sensitive to aniline vapor. Upon exposure to 0.1 ppm of aniline, a significant decrease in photocurrent (3%) was observed. Considering the fact that a well-shielded electrical measuring unit can detect a current change as small as below 0.1%, the nanofibril system shown in Fig. 3 can already detect aniline down to ppb and even sub ppb levels. Moreover, the photocurrent response to aniline vapor is reversible, facilitating the practical application of the sensing system.

The vapor sensing with the nanofibers was also tested against the common organic reagents, as shown in Fig. 3B, aiming to verify the sensing selectivity towards amines. Despite the much higher vapor pressure, the photoresponse observed for the organic vapors was much smaller than that observed for aniline. Moreover, the photocurrent change upon exposure to common organic vapors can be recovered completely within 30 s. Such rapid fluctuation in current is likely due to the surface desorption of oxygen caused by blowing of the organic vapor. Due to the weak physical adsorption of these organic species on the nanofiber, they can be quickly replaced by oxygen upon re-equilibration with air, thus recovering the photoconductivity. In comparison, the recovery of photocurrent after exposure to aniline vapor was in the time range of 10 min or longer, which is apparently attributed to the strong binding between amine and the positively charged nanofiber (under irradiation). The much

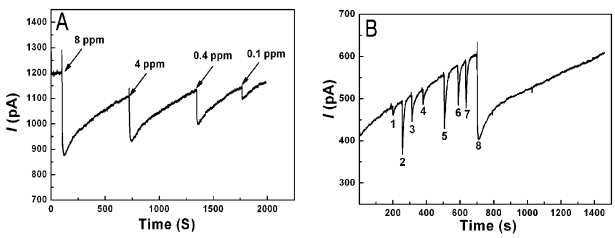

Fig. 3 (A) Photocurrent change of TDTC nanofibers upon exposure to aniline vapor at various pressures; (B) photocurrent change measured over the same nanofibers upon exposure to common organic vapors at high vapor pressures: (1) chloroform, 3500 ppm; (2) acetone, 4100 ppm (3); hexane: 2600 ppm (4) toluene, 750 ppm; (5) THF, 3500 ppm; (6) ethanol, 1500 ppm; (7) nitromethane, 1400 ppm. The response to aniline vapor at 25 ppm (8) is shown for comparison.

slower recovery of current thus observed for the aniline can be used as a signature (*via* digital differentiation, Fig. S8) for selective detection of amines against the common organic vapors.

In conclusion, we have fabricated p-type organic nanofibers from a tetracyclic macromolecule. High photoconductivity was achieved for these nanofibers though a simple photodoping process under ambient conditions. The high photoconductivity obtained for the nanofibers, combined with their intrinsic high surface area and porosity, enables efficient electrical vapor sensing of organic amines.

This work was supported by NSF (CAREER CHE 0641353, CBET 730667), DHS (2009-ST-108-LR0005), USTAR Program, DOE BES DEFG02-01ER45923.

Notes and references

1 D. Li, J. Huang and R. B. Kaner, *Acc. Chem. Res.*, 2009, **42**, 135.
2 Y. Che, X. Yang, S. Loser and L. Zang, *Nano Lett.*, 2008, **8**, 2219–2223.
3 T. Naddo, Y. Che, W. Zhang, K. Balakrishnan, X. Yang, M. Yen, J. Zhao, J. S. Moore and L. Zang, *J. Am. Chem. Soc.*, 2007, **129**, 6978–6979.
4 Y. Xia, P. Yang, Y. Sun, Y. Wu, B. Mayers, B. Gates, Y. Yin, F. Kim and H. Yan, *Adv. Mater.*, 2003, **15**, 353–389.
5 L. Zang, Y. Che and J. S. Moore, *Acc. Chem. Res.*, 2008, **41**, 1596–1608.
6 D. S. Weiss and M. Abkowitz, *Chem. Rev.*, 2010, **110**, 479–526.
7 Y. Yamamoto, T. Fukushima, Y. Suna, N. Ishii, A. Saeki, S. Seki, S. Tagawa, M. Taniguchi, T. Kawai and T. Aida, *Science*, 2006, **314**, 1761–1764.
8 Y. He, Y. Yamamoto, W. Jin, T. Fukushima, A. Saeki, S. Seki, N. Ishii and T. Aida, *Adv. Mater.*, 2010, **22**, 829–832.
9 A. D. Schwab, D. E. Smith, B. Bond-Watts, D. E. Johnston, J. Hone, A. T. Johnson, J. C. dePaula and W. F. Smith, *Nano Lett.*, 2004, **4**, 1261–1265.
10 X. Zhang, J. Jie, W. Zhang, C. Zhang, L. Luo, Z. He, X. Zhang, W. Zhang, C. Lee and S. Lee, *Adv. Mater.*, 2008, **20**, 2427–2432.
11 L. Jiang, Y. Fu, H. Li and W. Hu, *J. Am. Chem. Soc.*, 2008, **130**, 3937.
12 K. Balakrishnan, A. Datar, W. Zhang, X. Yang, T. Naddo, J. Huang, J. Zuo, M. Yen, J. S. Moore and L. Zang, *J. Am. Chem. Soc.*, 2006, **128**, 6576–6577.
13 A. J. Maliakal, J. Y. C. Chen, W.-Y. So, S. Jockusch, B. Kim, M. F. Ottaviani, A. Modelli, N. J. Turro, C. Nuckolls and A. P. Ramirez, *Chem. Mater.*, 2009, **21**, 5519.
14 M. S. A. Abdou, F. P. Orfino, Z. W. Xie, M. J. Deen and S. Holdcroft, *Adv. Mater.*, 1994, **6**, 838–841.
15 M. S. A. Abdou, F. P. Orfino, Y. Son and S. Holdcroft, *J. Am. Chem. Soc.*, 1997, **119**, 4518–4524.